Journal of Zhejiang University-SCIENCE A (Applied Physics & Engineering)
ISSN 1673-565X (Print); ISSN 1862-1775 (Online)
www.zju.edu.cn/jzus; www.springerlink.com
E-mail: jzus@zju.edu.cn

Preparation of $Cu/ZnO/Al_2O_3$ catalysts in a solvent-free routine for CO hydrogenation*

Hong LEI[1,2], Ren-feng NIE[1], Jin-hua FEI[1], Zhao-yin HOU[†‡1]

([1]*Institute of Catalysis, Department of Chemistry, Zhejiang University, Hangzhou 310028, China*)

([2]*College of Chemical and Material Engineering, Quzhou University, Quzhou 324000, China*)

[†]E-mail: zyhou@zju.edu.cn

Received Dec. 19, 2011; Revision accepted Mar. 13, 2012; Crosschecked Mar. 26, 2012

Abstract: The synthesis of methanol and dimethyl ether (DME) from CO hydrogenation has been investigated on Cu-based catalysts. A series of $Cu/ZnO/Al_2O_3$ catalysts were prepared using a solvent-free routine which involved a direct blend of copper/zinc/aluminum salts and citric acid, followed by calcination at 450 °C. The calcination processes were monitored using thermogravimetry differential scanning calorimetry (TG-DSC). Catalysts were further characterized using N_2 adsorption, scanning electronic microscopy (SEM), X-ray diffraction (XRD), N_2O oxidation followed by H_2 titration, and temperature-programmed reduction with H_2 (H_2-TPR). The reduction processes were also monitored with in-situ XRD. The physicochemical properties of catalysts depended strongly on the types of precursor salts, and catalysts prepared using Al acetate and Cu nitrate as starting materials had a larger surface area, larger exposed metallic copper surface area, and lower reduction temperature. The CO hydrogenation performances of these catalysts were compared and discussed in terms of their structures. Catalysts prepared with copper nitrate, zinc and aluminum acetates exhibited the highest catalytic activity.

Key words: $Cu/ZnO/Al_2O_3$ catalyst, Solvent-free routine, CO hydrogenation, Methanol, Dimethyl ether
doi:10.1631/jzus.A1100345 **Document code:** A **CLC number:** O643

1 Introduction

Production of methanol and dimethyl ether (DME) from CO hydrogenation has attracted much attention in recent years (Fei *et al*., 2006; Jin *et al*., 2007; Venugopal *et al*., 2009; Wang *et al*., 2009; Kang *et al*., 2010), since these compounds are interesting renewable energy sources with a high potential to minimize greenhouse gas emissions, thereby mitigating global warming (Fei *et al*., 2006; Bae *et al*., 2009; Gao *et al*., 2009). Methanol is a common feedstock for several important chemicals (Yang *et al*., 2008; Wang *et al*., 2010; Zhang *et al*., 2011). DME is also an important ingredient for the production of a wide range of chemicals such as dimethyl sulfate, methyl acetate, and light olefins (Bae *et al*., 2009; Gao *et al*., 2009). At the same time, both methanol and DME are safe mediums for the storage and transportation of hydrogen, and they are recommended as alternative fuels that can be directly used in fuel cells (Qi *et al*., 2001; Weng *et al*., 2005; Semelsberger *et al*., 2006; Teng, 2008).

$Cu/ZnO/Al_2O_3$ catalysts have been widely used for methanol and DME synthesis from CO hydrogenation because of their high catalytic activity, long lifetime, high poison resistance, and relatively low reaction temperature and pressure (Zhang *et al*., 1997; Reubroycharoen *et al*., 2004; Mao *et al*., 2005; Baltes *et al*., 2008; Behrens, 2009; Yang *et al*., 2010). Finding a better catalyst for methanol and DME synthesis is nevertheless still a subject of intense investigation. In order to increase the activity and stability of $Cu/ZnO/Al_2O_3$, a series of additives such as Zr, Y, La, and Ga are introduced to improve its performance for

‡ Corresponding author

* Project supported by the National Natural Science Foundation of China (Nos. 21073159 and 90610002), the National Basic Research Program (973) of China (No. 2007CB210207), and the Zhejiang Provincial Natural Science Foundation of China (No. Z406142)

CO hydrogenation to methanol and DME (Fei *et al*., 2006; Jin *et al*., 2007; Venugopal *et al*., 2009).

Preparation methods also play a crucial role in the catalytic performance of $Cu/ZnO/Al_2O_3$ (Hong *et al*., 2002; Liu *et al*., 2003; Arena *et al*., 2007). Numerous technical methods, such as co-precipitation (Zhang *et al*., 1997; Reubroycharoen *et al*., 2004; Mao *et al*., 2005; Baltes *et al*., 2008; Behrens, 2009; Yang *et al*., 2010; Behrens *et al*., 2011), impregnation (Choi *et al*., 2001), sol-gel (Wang *et al*., 2009; Fan *et al*., 2010), and reverse microemulsion techniques (Agrell *et al*., 2003) have been reported to prepare Cu/Zn/Al mixed oxide catalysts. Among these techniques, co-precipitation via hydroxycarbonate precursors followed by calcination is practical for commercial production of well-mixed $Cu/ZnO/Al_2O_3$ catalysts (Yang *et al*., 2008; Bae *et al*., 2009; Gao *et al*., 2009; Venugopal *et al*., 2009). However, co-precipitation often has disadvantages, such as time-consuming, tedious multistep processing, and delicate pH/temperature control (Castricum *et al*., 2001; Avgouropoulos and Ioannided, 2003; Wang *et al*., 2007; Guo *et al*., 2010). In addition, the final material obtained by the alkali co-precipitation route suffers from alkaline metal contamination as well as the formation of vast amounts of environmental waste (Wang *et al*., 2007).

The mechanical milling method and combustion synthesis method have been reported in the synthesis of various nanostructured metal and metal-oxide phases (Wang *et al*., 2007; Gu *et al*., 2009; Guo *et al*., 2010). The highly non-equilibratory nature of the mechanical milling process may provide a unique opportunity to prepare catalytic materials with improved physical and chemical properties (Trovarelli *et al*., 1997; Boldyrev and Tkáčová, 2000). Moreover, mechanical milling can be easily done under a solvent-free condition and rapidly produce large numbers of well-mixed catalysts. The combustion synthesis method, based on the principles of propellant chemistry, has been an attractive technique for the synthesis of metal oxide powders in recent years due to its low cost, precise stoichiometric ratio, and short reaction time (Ribeiro *et al*., 2008; Guo *et al*., 2010; Reddy *et al*., 2011). In the combustion synthesis process, a thermally induced redox reaction takes place between an oxidant and a fuel. In general, the metal nitrates are used as oxidants, whereas organic compounds such as citric acid, urea, and glycine are applied as fuels (Guo *et al*., 2010).

In this paper, we reported an easy solvent-free synthesis of $Cu/ZnO/Al_2O_3$ catalysts prepared using nitrate or acetate as metal precursors and citric acid as fuel via the mechanical milling and combustion synthesis method. The calcination processes were monitored using thermogravimetry differential scanning calorimetry (TG-DSC). The final catalysts were further characterized using N_2 adsorption, scanning electronic microscopy (SEM), X-ray diffraction (XRD), in-situ XRD, N_2O oxidation followed by H_2 titration, and temperature-programmed reduction with H_2 (H_2-TPR). Our objective was to combine the advantages of the mechanical milling method with those of combustion synthesis method. Special attention was paid to the effects of the Cu/Zn/Al precursor salts on their structures and catalytic behaviors in the methanol and DME synthesis from CO hydrogenation. The results of the physicochemical characterization are discussed in relation to the catalytic performances of $Cu/ZnO/Al_2O_3$ catalysts.

2 Experimental

2.1 Catalysts preparation

Six $Cu/ZnO/Al_2O_3$ samples (all with a Cu/Zn/Al atomic ratio of 60/25/15) were prepared using different copper/zinc/aluminum precursors and citric acid using the mechanical milling and combustion synthesis method. The composition of precursors is listed in Table 1. A typical procedure for preparing CZA-NNN catalyst is as follows: 14.50 g of $Cu(NO_3)_2{\cdot}3H_2O$, 7.44 g of $Zn(NO_3)_2{\cdot}6H_2O$, 5.63 g of $Al(NO_3)_3{\cdot}9H_2O$, and 19.21 g of citric acid were first premixed by hand for 1 h. The mixed powder was then loaded into an agate vial (50 ml) with agate milling balls under air atmosphere. The weight ratio between the balls and powders was kept at 10:1. The milling was carried out in a planetary mill (XQM-L, China) at 300 r/min for 2 h. After completion of milling, the resulting mixture was separated from the balls, followed by calcination at 450 °C for 4 h. The final sample was designated as CZA-NNN. The procedures for preparing CZA-ANN, CZA-NAN, CZA-NNA, CZA-NAA, and CZA-AAA catalysts were similar to that of CZA-NNN, but with different precursor salts (Table 1).

Table 1 Composition of the precursors of different Cu/Zn/Al_2O_3 catalysts

Catalyst	Copper salt	Zinc salt	Aluminum salt	Fuel
CZA-NNN	$Cu(NO_3)_2{\cdot}3H_2O$	$Zn(NO_3)_2{\cdot}6H_2O$	$Al(NO_3)_3{\cdot}9H_2O$	$C_6H_8O_7$
CZA-ANN	$Cu(CH_3COO)_2{\cdot}H_2O$	$Zn(NO_3)_2{\cdot}6H_2O$	$Al(NO_3)_3{\cdot}9H_2O$	$C_6H_8O_7$
CZA-NAN	$Cu(NO_3)_2{\cdot}3H_2O$	$Zn(CH_3COO)_2{\cdot}2H_2O$	$Al(NO_3)_3{\cdot}9H_2O$	$C_6H_8O_7$
CZA-NNA	$Cu(NO_3)_2{\cdot}3H_2O$	$Zn(NO_3)_2{\cdot}6H_2O$	$Al(CH_3COO)_3$	$C_6H_8O_7$
CZA-NAA	$Cu(NO_3)_2{\cdot}3H_2O$	$Zn(CH_3COO)_2{\cdot}2H_2O$	$Al(CH_3COO)_3$	$C_6H_8O_7$
CZA-AAA	$Cu(CH_3COO)_2{\cdot}H_2O$	$Zn(CH_3COO)_2{\cdot}2H_2O$	$Al(CH_3COO)_3$	$C_6H_8O_7$

2.2 Characterization

TG-DSC was carried out on a thermo-balance (Netzsch STA 409, Germany). Analysis was performed from 30 °C to 530 °C at a heating rate of 10 °C/min under N_2 flow (30 ml/min). N_2 adsorption was measured at its normal boiling point (−196 °C) using a volumetric adsorption analyzer (ASAP 2010, Micromeritics, US) after samples were pretreated at 250 °C for 4 h in vacuum. BET surface area was calculated on an adsorption branch.

XRD analysis was carried out on a Rigaku D/MAX-2500 diffractometer (Japan) with a scanning angle (2θ) of 15°–85° using Cu K_α radiation. In-situ XRD in H_2/Ar (volume ratio 1:10) flow at 30 ml/min was carried out on the same system connected to an Anton-Paar high temperature XRK assembly in which samples were mounted in a high-temperature cell, heated at 10 °C/min, and stabilized for 5 min before measurements. Cu particle sizes were calculated using Scherrer's equation.

SEM images of the calcined samples were obtained using a Leo Series VP 1430 microscope operating at 15 kV. Before being transferred into the SEM chamber, the samples dispersed with ethanol were deposited on the sample holder, and then quickly moved into the vacuum evaporator.

TPR experiments were conducted using H_2/N_2 (volume ratio 1:10) as a reducing gas in a quartz reactor. A freshly calcined catalyst of 20 mg was placed on top of glass wool in a quartz reactor and pretreated at 350 °C for 1 h under N_2 flow at 30 ml/min. After the sample was cooled to room temperature, the flow rate of the reducing gas was kept at 30 ml/min, with a ramp rate of 10 °C/min to a final temperature of 400 °C. The effluent gas was dried with KOH powder and the amount of hydrogen consumption was measured using a thermal conductivity detector (TCD).

The exposed metallic copper surface area (S_{Cu}) in the reduced catalyst was determined using the N_2O oxidation followed by H_2 titration as described in (Gervasini and Bennici, 2005; Yuan *et al*., 2011). The measurements were carried out in a linear quartz reactor. Catalysts were first reduced in the procedure described in the above TPR experiment until they reached 400 °C. The amount of hydrogen consumption in the first TPR was denoted as X. It was then purged with He and cooled to 50 °C. Surface copper atoms were oxidized in N_2O/N_2 (volume ratio 1:5) flow at 30 ml/min, 50 °C for 0.5 h. Finally, samples were flushed with He to remove the oxidants and cooled to room temperature to start another TPR run. Hydrogen consumption in the second TPR was denoted as Y. The dispersion of Cu and S_{Cu} were calculated using the following equations (Yuan *et al*., 2011).

All copper atoms were reduced in the first TPR:

$$CuO+H_2\rightarrow Cu+H_2O,$$
$$\text{Hydrogen consumption}=X.$$

Surface copper atoms oxidized to Cu_2O by N_2O at 50 °C were reduced in the second TPR:

$$Cu_2O+H_2\rightarrow 2Cu+H_2O,$$
$$\text{Hydrogen consumption}=Y.$$

And the dispersion of Cu and S_{Cu} were respectively calculated as:

$$D=(2\times Y/X)\times 100\%,$$
$$S_{Cu}=2\times Y\times N_{av}/(X\times M_{Cu}\times 1.4\times 10^{19})$$
$$=1353\times Y/X\ (m^2/g),$$

where N_{av} is the Avogadro's constant, M_{Cu} is the relative atomic mass of copper (63.456 g/mol), and 1.4×10^{19} is the copper atom surface density per square meter.

2.3 Catalyst reactions

Catalysts were evaluated in a continuous-flow, fixed-bed reactor. Catalyst of 2.0 g diluted with quartz sand (both in 20–40 meshes) was packed into the stainless steel tubular reactor. Prior to the activity test, all fresh catalysts were reduced under H_2 flow at 270 °C for 1 h under atmospheric pressure. Then, the reactor was cooled to 180 °C and the reactant gas flow was introduced. The reaction conditions employed in the activity test were temperature 260 °C, pressure 2.0 MPa, gas hourly space velocity (GHSV) 1500 h^{-1}, and a molar feed composition of CO/H_2=1/2. All post-reactor lines and valves were heated to 150 °C to prevent product condensation. The effluent products were analyzed on-line with a gas chromatograph equipped with a thermal detector, in which a Porapak-Q column was used to separate reaction products. Conversion and selectivity values were quoted as the average of three different analyses taken after 1 h of stream operation.

3 Results and discussion

3.1 Combustion and decomposition behaviors of the precursors

There are two steps involved in the formation of CZA catalysts with the mechanical milling and combustion synthesis method. First, complexes of metal-citrate were prepared using mechanical milling of metal salt and citric acid. Then, $CuO/ZnO/Al_2O_3$ was obtained by the combustion and decomposition of the Cu/Zn/Al citrate precursors (Behera *et al*., 2004). The combustion and decomposition behaviors of the precursors were recorded by TG-DSC. Fig. 1a shows that the combustion and thermal decomposition behavior of CZA-NNN proceeds in three stages. In the first stage, the weight loss of about 3.1% in the temperature range of 50–148 °C is attributed to the vaporization of physically absorbed water. In the second stage, the appearance of a weight loss of about 34.3% in the temperature range of 148–242 °C with a sharp exothermic peak around 180 °C is attributed to the combustion reaction between citric acid and nitrates. Finally, there is a weight loss of about 29.4% and a broad and small exothermic peak from 242–530 °C, which can be ascribed to the decomposition of the residual citric acid. As shown in Fig. 1a, the adoption of 450 °C as the calcination temperature can ensure a complete decomposition of the catalyst precursor. Although the low calcination temperature helps to decrease the sintering of copper, the residue will reduce the activity of the catalyst. Fig. 1b shows that the combustion and thermal decomposition behavior of CZA-ANN proceeds in four stages. In the second stage, a weight loss of about 17.4% in the temperature range of 150–226 °C with a sharp exothermic peak around 172 °C is attributed to the combustion reaction between citric acid and nitrates ($Zn(NO_3)_2$ and $Al(NO_3)_3$). The third stage shows an endothermic peak at 239 °C and a weight loss of 28.4%, which can be attributed to the decomposition of $Cu(CH_3COO)_2$ (Haynes and Lide, 2011). Figs. 1c–1e show that the combustion and thermal decomposition behaviors of CZA-NAN, CZA-NNA, and CZA-NAA also proceed in four steps. Fig. 1e shows a weight loss of about 16.6% in the temperature range of 130–210 °C with an exothermic peak around 157 °C, which is attributed to the combustion reaction between citric acid and copper nitrate. From 210 to 285 °C, there is a weight loss of about 27.1% and an endothermic peak around 244 °C, which can be ascribed to the decomposition of acetate ($Zn(CH_3COO)_2$ and $Al(CH_3COO)_3$). Fig. 1f shows that the combustion and thermal decomposition behavior of CZA-AAA proceeds in three stages. In the second stage, a weight loss of about 45.3% in the temperature range of 190–285 °C with a sharp endothermic peak around 242 °C is attributed to the decomposition of acetate ($Cu(CH_3COO)_2$, $Zn(CH_3COO)_2$, and $Al(CH_3COO)_3$). These observations unambiguously reveal that there are not combustion reactions between citric acid and acetate precursors, because the combustion reaction is a redox reaction which uses metal salts as oxidants and fuel as reductants (Fumo *et al*., 1996), and the acetate cannot oxidize citric acid. Comparisons of the TG-DSC profiles of catalysts prepared using different precursor salts reveal that the combustion temperature of CZA-NNN is the highest and that of CZA-NAA is the lowest. Copper acetate in CZA-ANN and CZA-AAA cannot combust with citric acid and needs to be decomposed at a higher temperature (239 °C). Therefore, the combustion processes depend strongly on the type of precursor salts.

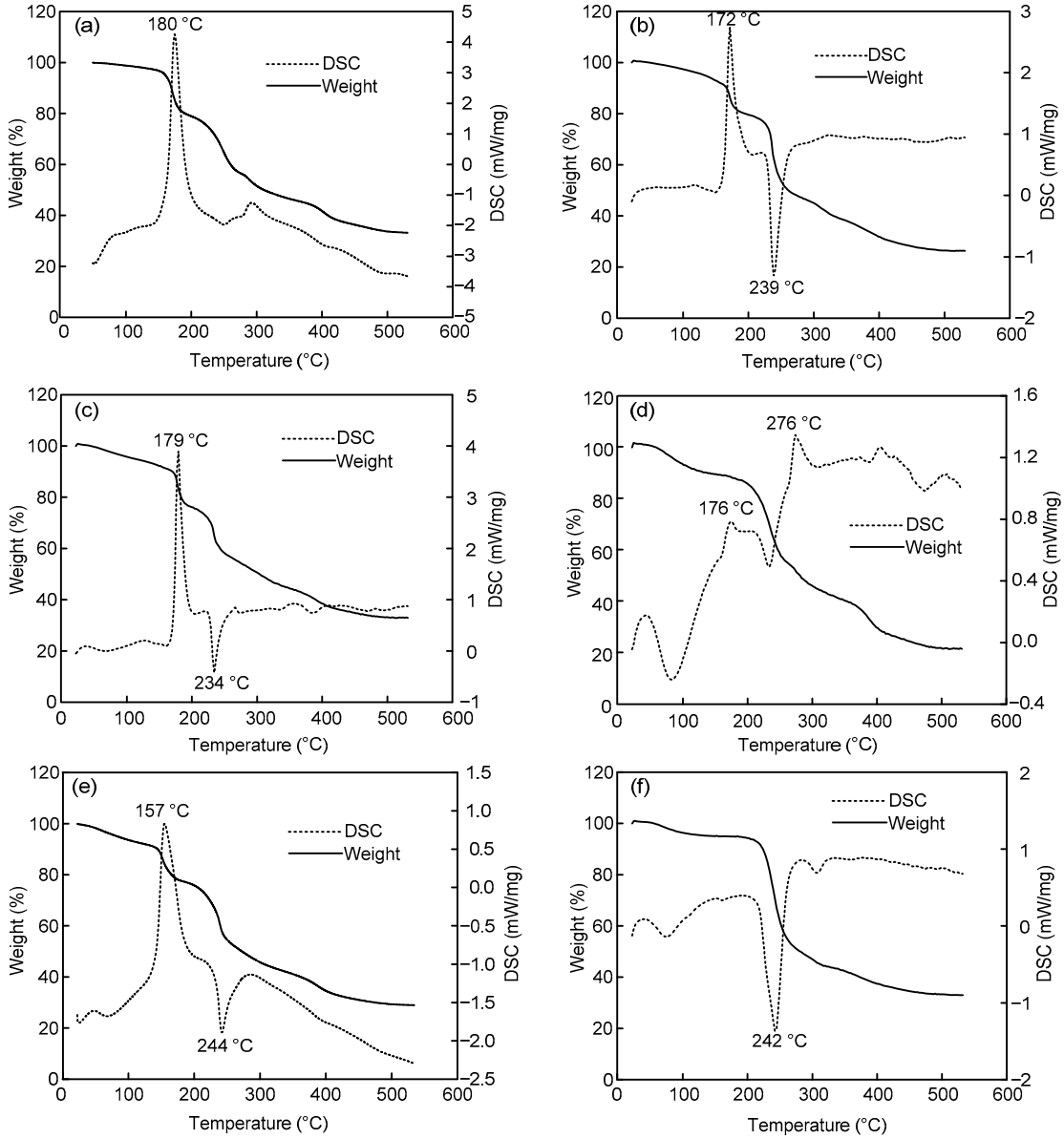

Fig. 1 TG-DSC of the Cu/Zn/Al mixed precursors

(a) CZA-NNN; (b) CZA-ANN; (c) CZA-NAN; (d) CZA-NNA; (e) CZA-NAA; (f) CZA-AAA

3.2 Structures of the calcined catalysts

The BET surface areas derived from nitrogen physisorption are summarized in Table 2. Catalysts prepared with aluminum acetate have larger surface areas than those obtained with aluminum nitrate where the same Cu/Zn precursor salts are used. Comparisons of the catalysts prepared with different copper salts and the same Zn/Al precursor salts reveal that the catalyst prepared using copper nitrate as a starting material has a larger surface area than the catalyst derived from copper acetate. The effects of the zinc salts on the surface areas of catalysts are opposite to those of copper salts. The maximum surface area is 67.4 m^2/g for CZA-NAA and the minimum surface area is 19.7 m^2/g for CZA-ANN. As mentioned above in the TG-DSC analysis, the combustion temperature of CZA-NAA is the lowest, and copper acetate in CZA-ANN cannot combust with citric acid and needs to be decomposed at higher temperatures. Lower combustion temperatures will result in higher surface area.

In order to inspect the reproducibility of surface areas of the catalysts, the CZA-NNN and CZA-ANN were prepared, again using the mechanical milling and combustion synthesis method. The surface areas of CZA-NNN and CZA-ANN are 32.9 and 19.6 m^2/g, respectively. Surface areas changed little during the second synthesis of catalysts, so the reproducibility of surface areas of the catalysts is good.

Table 2 Physicochemical properties of $Cu/ZnO/Al_2O_3$ catalysts prepared using the mechanical milling and combustion synthesis method

Catalyst	S_{BET} (m^2/g)	d_{Cu} (nm)	Dispersion (%)	S_{Cu} (m^2/g)
CZA-NNN	32.6	37.1	3.7	25.0
CZA-ANN	19.7		3.4	23.0
CZA-NAN	37.6		5.6	37.9
CZA-NNA	62.6		6.1	41.3
CZA-NAA	67.4	30.7	7.0	47.4
CZA-AAA	27.3		3.6	24.4

S_{BET} is the BET specific surface area; d_{Cu} is the particle size of Cu determined after reduction by the in-situ XRD data based on Scherrer's equation. The exposed metallic copper surface area (S_{Cu}) and dispersion in the reduced catalyst were determined by N_2O chemisorption at 50 °C using the procedure described in (Gervasini and Bennici, 2005; Yuan *et al*., 2011)

Fig. 2 shows the surface morphology of calcined catalysts. The samples obtained using aluminum nitrate afforded the massive agglomerates apparently larger than those samples prepared using aluminum acetate when the same Cu/Zn precursor salts were used. Tsubaki *et al*. (2010) reported that aluminum nitrate acted as the binder for zeolite membrane growth. In this experiment, aluminum nitrate may have promoted the growth of particles as binders during the preparation process of the catalyst. Moreover, as mentioned in the above TG-DSC analysis, the decomposition temperature of copper salts in catalysts prepared by aluminum nitrate under the same conditions is higher, and the high combustion temperature leads to sintering of particles. In contrast, the particles of calcined CZA-NNA and CZA-NAA prepared using aluminum acetate as a starting material are disk-like, and the distribution of the main particles for both catalysts seems to be uniform, with an average size of <300 nm. Grunwaldt *et al*. (2000) found that the morphology of copper particles was disk-like due to the strong interaction between Cu and ZnO. Comparisons of the catalysts prepared with different copper salts and the same Zn/Al precursor

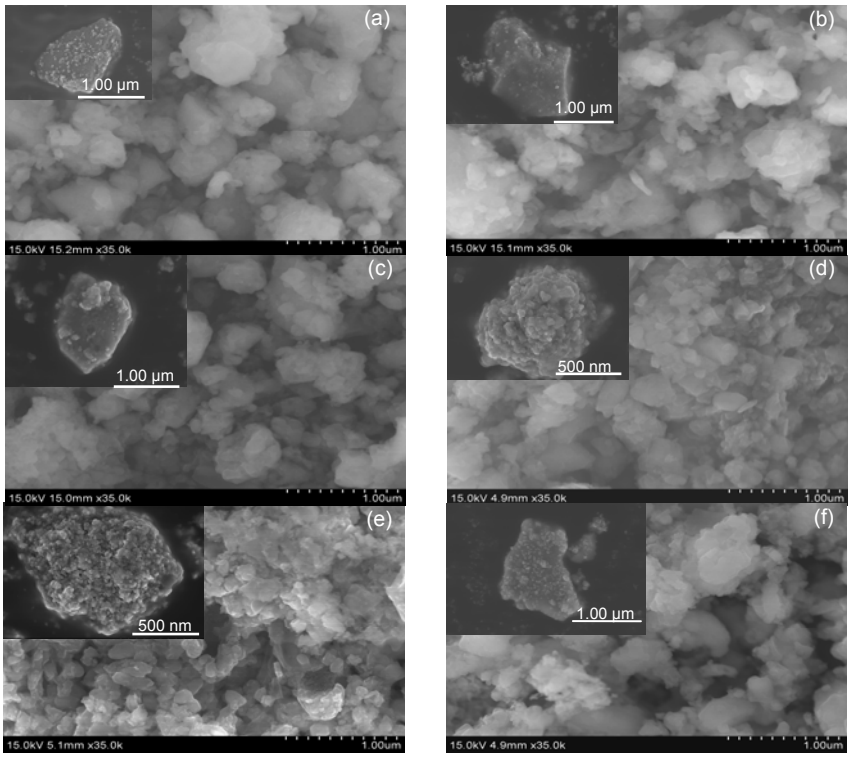

Fig. 2 SEM images of the catalysts prepared using the mechanical milling and combustion synthesis method
(a) CZA-NNN; (b) CZA-ANN; (c) CZA-NAN; (d) CZA-NNA; (e) CZA-NAA; (f) CZA-AAA

salts reveal that the catalyst prepared using copper nitrate as a starting material forms smaller particles than the catalyst derived from copper acetate. The effects of the zinc salts on the particle size of catalysts are opposite to those of copper salts. Therefore, SEM images of these catalysts suggest that copper nitrate, zinc acetate, and aluminum acetate are more effective than copper acetate, zinc nitrate, and aluminum nitrate in terms of the mechanical milling and combustion synthesis of $Cu/ZnO/Al_2O_3$ catalysts with high component distribution and small particle size. These results are in accordance with their surface areas.

SEM images of single particle of calcined catalysts show a clear change in morphology. As shown in the inserts of Figs. 2a–2c and 2f, CZA-NNN, CZA-ANN, CZA-NAN, and CZA-AAA exhibit a solid brick-like morphology with large particle size and are nonporous, which is consistent with their small surface areas. When aluminum acetate was used, the petal-like morphology for CZA-NNA (Fig. 2d) and the honeycomb morphology for CZA-NAA (Fig. 2e) with plenty of pore channels were observed, which was consistent with their large surface areas.

Fig. 3 compares the XRD patterns of calcined catalysts obtained by mechanical milling and combustion synthesis method. It can be seen that the diffraction lines of CuO (JCPDS 44-0706) appear at 2θ of 32.6°, 35.6°, 38.8°, and 48.9°. The diffraction lines of the ZnO phase (JCPDS 36-1451) are observed at 2θ of 31.8°, 34.5°, and 36.3°. The diffraction peaks of ZnO and CuO are not finely resolved. The broad reflections indicate that part of the Cu may be dissolved in the Zn matrix or the CuO phase is in intimate contact with ZnO (Venugopal *et al*., 2009). No diffraction peaks of the Al_2O_3 phase can be observed in the calcined catalysts. This is due to the fact that Al_2O_3 is present in small quantities and/or in amorphous state.

XRD patterns of CZA-NNN and CZA-NAA catalysts after reduction are shown in Fig. 4. The diffraction peaks of CuO in fresh calcined CZA-NNN and CZA-NAA catalysts disappear after reduction and only the metallic copper (2θ=43.1° and 50.2°) and ZnO phases can be seen for the two catalysts. Average copper metal crystallite sizes were calculated using Scherrer's equation from the full width half maximum of Cu (111) diffraction lines. The copper particle size of CZA-NAA (30.7 nm) is smaller than that of CZA-NNN (37.1 nm).

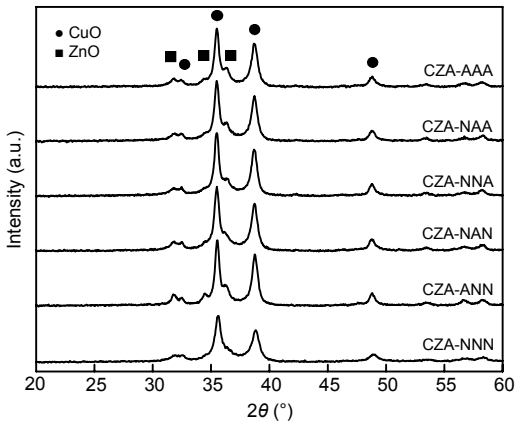

Fig. 3 XRD patterns of $CuO/ZnO/Al_2O_3$ catalysts prepared with different precursors

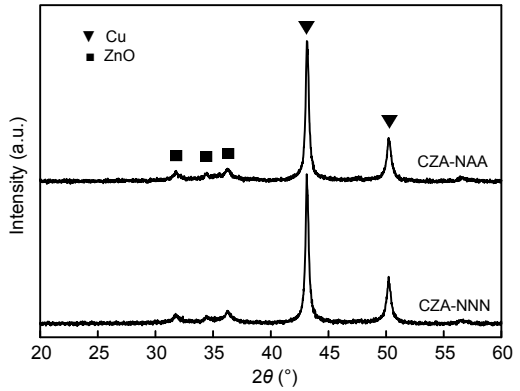

Fig. 4 XRD patterns of the CZA-NNN and CZA-NAA catalysts after reduction

The S_{Cu} in reduced catalysts were determined using N_2O oxidation followed by H_2 titration as described in Gervasini and Bennici (2005) and Yuan *et al*. (2011); these data are summarized in Table 2. The S_{Cu} of these reduced catalysts are in the range of 23.0–47.4 m^2/g. The catalysts prepared with aluminum acetate have a larger S_{Cu} than the catalysts derived from aluminum nitrate under the same Cu/Zn precursor salts. The catalysts obtained with zinc acetate have a larger S_{Cu} than catalysts derived from zinc nitrate where the same Cu/Al precursor salts were used. The S_{Cu} of the catalyst obtained with copper nitrate is larger than that of the catalyst derived from copper acetate. CZA-NAA has the largest S_{Cu} (47.4 m^2/g), which can be explained by the low decomposition temperature of copper salt.

As reported in (Zhang and Gao, 2004; Guo *et al*., 2010), the structure of catalysts prepared via combustion was mainly determined by their combustion temperature. It is well known that low combustion

temperatures will result in small particle sizes, large surface area, and large exposed Cu surface area. The combustion temperature of CZA-NNN is the highest and that of CZA-NAA is the lowest. The small surface area and the small Cu surface area of CZA-ANN and CZA-AAA can be attributed to the higher decomposition temperature of copper acetate, which cannot combust with citric acid and need to be decomposed at higher temperatures. We conclude that surface area, particle size, and Cu surface area of prepared catalysts depend strongly on the type of precursor salts.

3.3 Reducibility of catalyst

As shown in Fig. 5, the reduction profiles of all samples prepared with different precursor salts with the mechanical milling and combustion synthesis method exhibit two peaks of H_2 consumption below 300 °C; these are denoted as α and β peaks and attributed to the reduction of two different types of CuO phase. The low temperature peak (α peak) is attributed to the reduction of highly dispersed CuO that strongly interacting with ZnO and Al_2O_3, whereas the peak appearing at the higher temperature (β peak) is due to the reduction of bulk CuO (Gunter *et al*., 2001; Wang *et al*., 2007). Copper oxide species in CZA catalysts were reduced at much lower temperatures compared with pure bulk CuO which was reported to be reduced at 340 °C (Wang *et al*., 2007). These results indicate that ZnO and Al_2O_3 can promote the dispersion of copper oxide and enhance the reducibility of copper phase (Zhang *et al*., 2006). Catalysts prepared via aluminum acetate display a lower reduction temperature than catalysts prepared via aluminum nitrate when the same Cu/Zn precursor salts were used, and catalysts prepared via zinc acetate have a lower reduction temperature than catalysts prepared via zinc nitrate when the same Cu/Al precursor salts are used. The effects of the copper salts on the reducibility of the catalyst are opposite to those of the aluminum salts. These results are consistent with the decomposition temperature of precursor salts. The CZA-ANN catalyst has the highest reduction peaks at 223 °C with a shoulder peak at 266 °C. The CZA-NAA catalyst displays the lowest reduction peak at 191 °C with a shoulder peak at 241 °C, which indicates the presence of small CuO particles and a high CuO dispersion. These results also correlate well with the exposed metallic copper surface area.

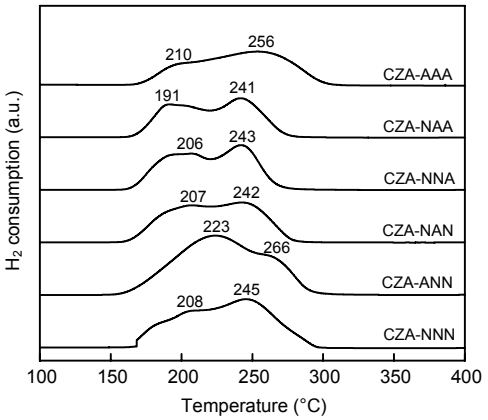

Fig. 5 H_2-TPR profiles of CuO/ZnO/Al_2O_3 catalysts prepared with different precursors

Fig. 6 shows in-situ XRD spectra of the H_2 reduction process of CZA-NNN and CZA-NAA under H_2/Ar (volumn ratio 1:10) flow at 30 ml/min. As shown in Fig. 6a, the intensity of the diffraction lines of CuO in CZA-NNN decreased gradually from 190 °C to 250 °C, which indicates that the size of CuO particles decreased as the reduction of CuO started. When the temperature exceeded 280 °C, the diffraction lines of CuO disappeared and the diffraction lines of Cu appeared. The intensity of the diffraction lines of CuO in CZA-NAA decreased gradually from 180 °C to 250 °C and the diffraction lines of Cu appeared at 250 °C. These results indicate that CZA-NAA has lower reduction temperature compared with CZA-NNN, which is consistent with the TPR results. Thus, Cu particle size is correlated with the induction factor for the reduction process. The Cu (111) diffraction lines (2θ=43.1°) of CZA-NNN and CZA-NAA shift slightly at a lower angle compared with the Cu (111) diffraction line (2θ=43.3°) of pure Cu, which suggests that part of the Zn may be dissolved in the Cu matrix (Liu *et al*., 2011).

3.4 Catalytic performance

The catalytic activities of these catalysts for CO hydrogenation to methanol and DME are presented in Table 3. The CZA-NAA catalyst exhibits the best activity (60.0% conversion rate of CO) and selectivity of methanol and DME reaches 10.2% and 59.0%, respectively, possibly because it has the largest surface area and the largest copper surface area. The conversion of CO decreases to 47.5% and 21.1% over CZA-NNA and CZA-NNN. CZA-ANN shows the

Table 3 CO hydrogenation performance of $CuO/ZnO/Al_2O_3$ catalysts prepared using mechanical milling and combustion synthesis

Catalyst	CO conversion rate (%)	Selectivity (%)				
		Methanol	DME	CO_2	CH_4	C_2H_6
CZA-NNN	21.1	12.1	17.6	45.2	16.2	8.9
CZA-ANN	17.6	21.7	17.7	35.6	17.3	7.7
CZA-NAN	23.8	28.1	26.0	28.1	10.6	7.2
CZA-NNA	47.5	11.6	58.9	23.0	4.1	2.4
CZA-NAA	60.0	10.2	59.0	24.3	3.8	2.7
CZA-AAA	19.6	39.2	5.6	33.4	13.9	7.9

Reaction conditions: molar feed composition of H_2:CO=2:1, temperature of 260 °C, pressure of 2.0 MPa, and GHSV of 1500 h^{-1}

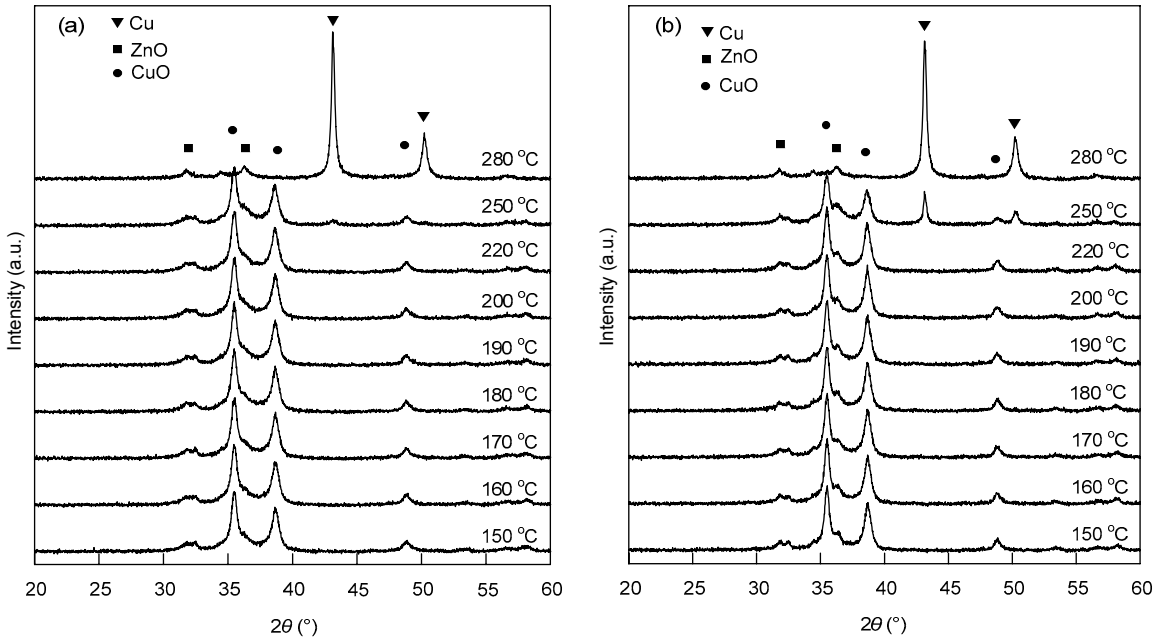

Fig. 6 In-situ XRD of the calcined CZA-NNN catalyst (a) and CZA-NAA catalyst (b) at different temperatures in H_2/N_2 (volume ratio 1:10) flow at 30 ml/min

lowest activity with a 17.6% CO conversion, 21.7% selectivity of methanol, and 17.7% selectivity of DME due to its small surface area and small exposed copper surface area. These results indicate that: (1) the catalytic activity of the catalysts prepared by aluminum acetate is higher than that of the catalysts prepared with aluminum nitrate when the same Cu/Zn precursor salts are used; (2) the effect of zinc salt on the catalytic activity of catalysts is similar to that of aluminum salt; and, (3) the effect of copper salt on the catalytic activity of catalysts is opposite to that of aluminum salt. These results correlate well with their physicochemical properties. Table 3 shows that the catalytic activities of catalysts prepared with copper nitrate are higher than those of catalysts obtained with copper acetate, which indicates that catalysts prepared using the combustion synthesis method have higher activity due to the lower decomposition temperature of copper salt.

The stability of the most efficient CZA-NAA catalyst for CO hydrogenation to produce methanol and DME was measured over a 120-h period, during which time the reactor operated continuously under the test conditions. As shown in Fig. 7, the CO conversion rate and the selectivity for methanol and DME decreased by less than 4% and 2% from their initially stabilized values, respectively. It is clear that the CZA-NAA sample prepared by the mechanical milling and combustion synthesis method exhibits a stable catalytic performance in the whole test period.

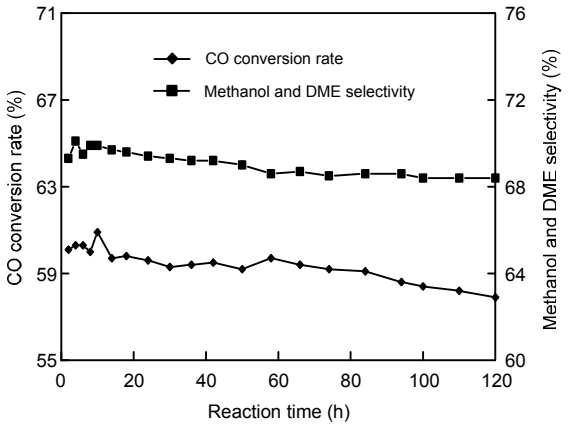

Fig. 7 Variation of CO conversion rate, methanol and DME selectivity with reaction time over CZA-NAA catalyst
Reaction conditions: molar feed composition of H_2:CO=2:1, temperature of 260 °C, pressure of 2.0 MPa, and GHSV of 1500 h^{-1}

4 Conclusions

A series of $Cu/ZnO/Al_2O_3$ catalysts were prepared using citric acid as fuel and different copper, zinc, and aluminum salts as precursor salts via the mechanical milling and combustion synthesis method. The combustion processes and physicochemical properties of catalysts depended strongly on the type of precursor salts and the decomposition temperature of copper salt. $Cu/ZnO/Al_2O_3$ catalysts prepared using Al acetate and Cu nitrate have larger surface area, larger exposed Cu metal surface area, and lower reduction temperature due to the low decomposition temperature of copper salt; these catalysts exhibited the highest activity for CO hydrogenation. Mechanical milling and combustion synthesis based on dry precursor salts provides an attractive method for the environmentally friendly and energy-efficient fabrication of $Cu/ZnO/Al_2O_3$ catalysts that are highly effective in the production of methanol and DME from CO hydrogenation.

References

Agrell, J., Boutonnet, M., Fierro, J.L.G., 2003. Production of hydrogen from methanol over binary Cu/ZnO catalysts: Part II. Catalytic activity and reaction pathways. *Applied Catalysis A: General*, **253**(1):213-223. [doi:10.1016/S0926-860X(03)00521-0]

Arena, F., Barbera, K., Italiano, G., Bonura, G., Spadaro, L., Frusteri, F., 2007. Synthesis, characterization and activity pattern of Cu-ZnO/ZrO_2 catalysts in the hydrogenation of carbon dioxide to methanol. *Journal of Catalysis*, **249**(2):185-194. [doi:10.1016/j.jcat.2007.04.003]

Avgouropoulos, G., Ioannided, T., 2003. Selective CO oxidation over CuO-CeO_2 catalysts prepared via the urea-nitrate combustion method. *Applied Catalysis A: General*, **244**(1):155-167. [doi:10.1016/S0926-860X(02)00558-6]

Bae, J.W., Kang, S.H., Lee, Y.J., Jun, K.W., 2009. Synthesis of DME from syngas on the bifunctional Cu-ZnO-Al_2O_3/Zr-modified ferrierite: effect of Zr content. *Applied Catalysis B: Environmental*, **90**(3-4):426-435. [doi:10.1016/j.apcatb.2009.04.002]

Baltes, C., Vukojević, S., Schüth, F., 2008. Correlations between synthesis, precursor, and catalyst structure and activity of a large set of CuO/ZnO/Al_2O_3 catalysts for methanol synthesis. *Journal of Catalysis*, **258**(2):334-344. [doi:10.1016/j.jcat.2008.07.004]

Behera, S.K., Barpanda, P., Pratihar, S.K., Bhattacharyya, S., 2004. Synthesis of magnesium-aluminium spinel from autoignition of citrate-nitrate gel. *Materials Letters*, **58**(9):1451-1455. [doi:10.1016/j.matlet.2003.10.004]

Behrens, M., 2009. Meso- and nano-structuring of industrial Cu/ZnO/(Al_2O_3) catalysts. *Journal of Catalysis*, **267**(1):24-29. [doi:10.1016/j.jcat.2009.07.009]

Behrens, M., Kiner, S., Girsgdies, F., Kasatkin, I., Hermerschmitdt, F., Mette, K., Ruland, H., Muhler, M., Schlögl, R., 2011. Knowledge-based development of a nitrate-free synthesis route for Cu/ZnO methanol synthesis catalysts via formate precursors. *Chemical Communications*, **47**(6):1701-1703. [doi:10.1039/C0CC04933F]

Boldyrev, V.V., Tkáčová, K., 2000. Mechanochemistry of solids: past, present, and prospects. *Journal of Materials Synthesis and Processing*, **8**(3-4):121-132. [doi:10.1023/A:1011347706721]

Castricum, H.L., Bakker, H., Poels, E.K., 2001. Oxidation and reduction in copper/zinc oxides by mechanical milling. *Materials Science and Engineering: A*, **304-306**:418-423. [doi:10.1016/S0921-5093(00)01485-4]

Choi, Y., Futagami, K., Fujitani, T., Nakamura, J., 2001. The role of ZnO in Cu/ZnO methanol synthesis catalysts—morphology effect or active site model. *Applied Catalysis A: General*, **208**(1-2):163-167. [doi:10.1016/S0926-860X(00)00712-2]

Fan, J.C., Chen, C.Q., Zhao, J., Huang, W., Xie, K.C., 2010. Effect of surfactant on structure and performance of catalysts for DME synthesis in slurry bed. *Fuel Processing Technology*, **91**(4):414-418. [doi:10.1016/j.fuproc.2009.05.005]

Fei, J.H., Hou, Z.Y., Zhu, B., Lou, H., Zheng, X.M., 2006. Synthesis of dimethyl ether (DME) on modified HY zeolite and modified HY zeolite-supported Cu-Mn-Zn catalysts. *Applied Catalysis A: General*, **304**:49-54. [doi:10.1016/j.apcata.2006.02.019]

Fumo, D.A., Morelli, M.R., Segadães, A.M., 1996. Combustion synthesis of calcium aluminates. *Materials Research Bulletin*, **31**(10):1243-1255. [doi:10.1016/0025-5408(96)00112-2]

Gao, Z.H., Huang, W., Yin, L.H., Xie, K.C., 2009.

Liquid-phase preparation of catalysts used in slurry reactors to synthesize dimethyl ether from syngas: effect of heat-treatment atmosphere. *Fuel Processing Technology*, **90**(12):1442-1446. [doi:10.1016/j.fuproc.2009.06.022]

Gervasini, A., Bennici, S., 2005. Dispersion and surface states of copper catalysts by temperature-programmed-reduction of oxidized surfaces (s-TPR). *Applied Catalysis A: General*, **281**(1-2):199-205. [doi:10.1016/j.apcata.2004.11.030]

Grunwaldt, J.D., Molenbroek, A.M., Topsoe, N.Y., Topsoe, H., Clausen, B.C., 2000. In situ investigations of structural changes in Cu/ZnO catalysts. *Journal of Catalysis*, **194**(2):452-460. [doi:10.1006/jcat.2000.2930]

Gu, H., Zhu, Y.F., Li, L.Q., 2009. Hydrogen storage properties of Mg-Ni-Cu prepared by hydriding combustion synthesis and mechanical milling (HCSDMM). *International Journal of Hydrogen Energy*, **34**(6):2654-2660. [doi:10.1016/j.ijhydene.2009.01.068]

Gunter, M.M., Ressler, T., Jentoft, R.E., Bems, B., 2001. Redox behavior of copper oxide/zinc oxide catalysts in the steam reforming of methanol studied by in situ X-ray diffraction and absorption spectroscopy. *Journal of Catalysis*, **203**(1):133-149. [doi:10.1006/jcat.2001.3322]

Guo, X.M., Mao, D.S., Lu, G.Z., Wang, S., Wu, G.S., 2010. Glycine-nitrate combustion synthesis of CuO-ZnO-ZrO_2 catalysts for methanol synthesis from CO_2 hydrogenation. *Journal of Catalysis*, **271**(2):178-185. [doi:10.1016/j.jcat.2010.01.009]

Haynes, W.M., Lide, D.R., 2011. CRC Handbook of Chemistry and Physics. Chemical Rubber Co., Cleveland, US, p.44-101.

Hong, Z.S., Cao, Y., Deng, J.F., Fan, K.N., 2002. CO_2 hydrogenation to methanol over Cu/ZnO/Al_2O_3 catalysts prepared by a novel gel-network-coprecipitation method. *Catalysis Letters*, **82**(1-2):37-44. [doi:10.1023/A:1020531822590]

Jin, D.F., Zhu, B., Hou, Z.Y., Fei, J.H., Lou, H., Zheng, X.M., 2007. Dimethyl ether synthesis via methanol and syngas over rare earth metals modified zeolite Y and dual Cu-Mn-Zn catalysts. *Fuel*, **86**(17-18):2707-2713. [doi:10.1016/j.fuel.2007.03.011]

Kang, S.H., Bae, J.W., Kim, H.S., Dhar, G.M., Jun, K.W., 2010. Enhanced catalytic performance for dimethyl ether synthesis from syngas with the addition of Zr or Ga on a Cu-ZnO-Al_2O_3/γ-Al_2O_3 bifunctional catalyst. *Energy Fuels*, **24**(2):804-810. [doi:10.1021/ef901133z]

Liu, X.M., Lu, G.Q., Yan, Z.F., Beltramini, J., 2003. Recent advances in catalysts for methanol synthesis via hydrogenation of CO and CO_2. *Industrial & Engineering Chemistry Research*, **42**(25):6518-6530. [doi:10.1021/ie020979s]

Liu, X.Y., Wang, A.Q., Li, L., Zhang, T., Mou, C.Y., Lee, J.F., 2011. Structural changes of Au-Cu bimetallic catalysts in CO oxidation: in situ XRD, EPR, XANES, and FT-IR characterizations. *Journal of Catalysis*, **278**(2):288-296. [doi:10.1016/j.jcat.2010.12.016]

Mao, D.S., Yang, W.M., Xia, J.C., Zhang, B., Song, Q.Y., Chen, Q.L., 2005. Highly effective hybrid catalyst for the direct synthesis of dimethyl ether from syngas with magnesium oxide-modified HZSM-5 as a dehydration component. *Journal of Catalysis*, **230**(1):140-149. [doi:10.1016/j.jcat.2004.12.007]

Qi, G.X., Zheng, X.M., Fei, J.H., Hou, Z.Y., 2001. A novel catalyst for DME synthesis from CO hydrogenation: activity, structure and surface properties. *Journal of Molecular Catalysis A: Chemical*, **176**(1-2):195-203. [doi:10.1016/S1381-1169(01)00257-6]

Reddy, A.J., Kokila, M.K., Nagabhushana, H., Chakradhar, R.P.S., Shivakumara, C., Rao, J.L., Nagabhushana, B.M., 2011. Structural, optical and EPR studies on ZnO:Cu nanopowder prepared via low temperature solution combustion synthesis. *Journal of Alloys and Compounds*, **509**(17):5349-5355. [doi:10.1016/j.jallcom.2011.02.043]

Reubroycharoen, P., Vitidsant, T., Yoneyama, Y., Tsubaki, N., 2004. Development of a new low-temperature methanol synthesis process. *Catalysis Today*, **89**(4):447-454. [doi:10.1016/j.cattod.2004.01.006]

Ribeiro, N.F.P., Souza, M.M.V.M., Schmal, M., 2008. Combustion synthesis of copper catalysts for selective CO oxidation. *Journal of Power Sources*, **179**(1):329-334. [doi:10.1016/j.jpowsour.2007.12.096]

Semelsberger, T.A., Borup, R.L., Greene, H.L., 2006. Dimethyl ether (DME) as an alternative fuel. *Journal of Power Sources*, **156**(2):497-511. [doi:10.1016/j.jpowsour.2005.05.082]

Teng, L.H., 2008. Attrition resistant catalyst for dimethyl ether synthesis in fluidized-bed reactor. *Journal of Zhejiang University-SCIENCE A*, **9**(9):1288-1295. [doi:10.1631/jzus.A0820155]

Trovarelli, A., Zamar, F., Llorca, J., de Leitenburg, C., Dolcetti, G., Kiss, J.T., 1997. Nanophase fluorite-structured CeO_2-ZrO_2 catalysts prepared by high-energy mechanical milling. *Journal of Catalysis*, **169**(2):490-502. [doi:10.1006/jcat.1997.1705]

Venugopal, A., Palgunadi, J., Deog, J.K., Joo, O.S., Shin, C.H., 2009. Dimethyl ether synthesis on the admixed catalysts of Cu-Zn-Al-*M* (*M*=Ga, La, Y, Zr) and γ-Al_2O_3: the role of modifier. *Journal of Molecular Catalysis A: Chemical*, **302**(1-2):20-27. [doi:10.1016/j.molcata.2008.11.038]

Wang, D.S., Han, Y.Z., Tan, Y.S., Tsubaki, N., 2009. Effect of H_2O on Cu-based catalyst in one-step slurry phase dimethyl ether synthesis. *Fuel Processing Technology*, **90**(3):446-451. [doi:10.1016/j.fuproc.2008.11.007]

Wang, D.Y., Zhou, J., Liu, G.Z., 2009. The microstructure and photoluminescence of Cu-doped ZnO nano-crystal thin films prepared by sol-gel method. *Journal of Alloys and Compounds*, **487**(1-2):545-549. [doi:10.1016/j.jallcom.2009.08.011]

Wang, L.C., Liu, Y.M., Chen, M., Cao, Y., He, H.Y., Wu, G.S., Dai, W.L., Fan, K.N., 2007, Production of hydrogen by steam reforming of methanol over Cu/ZnO catalysts prepared via a practical soft reactive grinding route based on dry oxalate-precursor synthesis. *Journal of Catalysis*,

246(1):193-204. [doi:10.1016/j.jcat.2006.12.006]

Wang, L.L., Ding, W., Liu, Y.W., Fang, W.P., Yang, Y.Q., 2010. Effect of preparation methods of aluminum emulsions on catalytic on catalytic performance of copper-based catalysts for methanol synthesis from syngas. *Journal of Natural Gas Chemistry*, **19**(5):487-492. [doi:10.1016/S1003-9953(09)60105-5]

Wen, H., Liu, Y.C., Wei, M.R., 2005. Multidimensional modeling of dimethyl ether (DME) spray combustion in DI diesel engine. *Journal of Zhejiang University-SCIENCE A*, **6**(4):276-282. [doi:10.1631/jzus.2005.A0276]

Yang, G.H., Tsubaki, N., Shamoto, J., Yoneyama, Y., Zhang, Y., 2010. Confinement effect and synergistic function of H-ZSM-5/Cu-ZnO-Al_2O_3 capsule catalyst for one-step controlled synthesis. *Journal of the American Chemical Society*, **132**(23):8129-8136. [doi:10.1021/ja101882a]

Yang, R.Q., Yu, X.C., Zhang, Y., Li, W.Z., Tsubaki, N., 2008. A new method of low-temperature methanol synthesis on Cu/ZnO/Al_2O_3 catalysts from CO/CO_2/H_2. *Fuel*, **87**(4-5):443-450. [doi:10.1016/j.fuel.2007.06.020]

Yuan, Z.L., Wang, L.N., Wang, J.H., Xia, S.X., Chen, P., Hou, Z.Y., Zheng, X.M., 2011. Hydrogenolysis of glycerol over homogenously dispersed copper on solid base catalysts. *Applied Catalysis B: Environmental*, **101**(3-4):431-440. [doi:10.1016/j.apcatb.2010.10.013]

Zhang, J.C., Zhang, H.B., Yang, X.Y., Huang, Z., Cao, W.L., 2011. Study on the deactivation and regeneration of the ZSM-5 catalyst used in methanol to olefins. *Journal of Natural Gas Chemistry*, **20**(3):266-270. [doi:10.1016/S1003-9953(10)60183-1]

Zhang, J.R., Gao, L., 2004. Antimony-doped tin oxide nanocrystallites prepared by a combustion process. *Materials Letters*, **58**(22-23):2730-2734. [doi:10.1016/j.matlet.2004.01.041]

Zhang, Y.L., Sun, Q., Deng, J.F., Wu, D., 1997. A high activity Cu/ZnO/Al_2O_3 catalyst for methanol synthesis: preparation and catalytic properties. *Applied Catalysis A: General*, **158**(1-2):105-120. [doi:10.1016/S0926-860X(96)00362-6]

Zhang, Y.P., Fei, J.H., Yu, Y.M., Zheng, X.M., 2006. Methanol synthesis from CO_2 hydrogenation over Cu based catalyst supported on zirconia modified γ-Al_2O_3. *Energy Conversion and Management*, **47**(18-19):3360-3367. [doi:10.1016/j.enconman.2006.01.010]